SPE 118906

Advanced Reservoir Management Workflow Using an EnKF Based Assisted History Matching Method

A. Seiler, G. Evensen, J.-A. Skjervheim, J. Hove, J.G. Vabø, StatoilHydro ASA

This paper was prepared for presentation at the 2009 SPE Reservoir Simulation Symposium held in the Woodlands, Texas, USA, 2-4 February 2009.

Abstract

This paper demonstrates the potential and advantages of the Ensemble Kalman filter (EnKF) as a tool for assisted history matching, based on its sequential processing of measurements, its capability of handling large parameter sets, and on the fact that it solves the combined state and parameter estimation problem.

A method and a thorough workflow for updating reservoir simulation models using the EnKF is developed. In addition, we present a method for updating relative permeability curves, as well as an improved approach for updating fault transmissibility multipliers.

The proposed workflow has been applied on a complex North Sea oil field. The EnKF successfully provides an ensemble of history matched reservoir models. A significant improvement in the history match is obtained by updating the relative permeability properties in addition to porosity and permeability fields and initial fluid contacts. Fault multipliers are estimated, and it is shown how the use of transformations, which handles non-Gaussian model variables, makes it possible to determine if a fault is open, closed, or partially closed with respect to flow.

The presented method is an innovative contribution to reservoir management workflows, which show growing interest in real time applications and fast model updating. Sequential data assimilation provides an updated reservoir model conditioned on the most recent production data. The updated ensemble is used to predict the uncertainty in future production and it is demonstrated that the EnKF leads to improved predictions with reduced uncertainty.

Introduction

Reservoir modelling and history matching aim to deliver integrated reservoir models for reservoir management purposes. These reservoir models must not only reproduce the historical field performances, they must also be consistent with all available static data (such as core data, well logs, seismic data) and dynamic data (such as well production data, tracer concentration, 4D seismic data). Furthermore they should integrate the most current information about the reservoir and the associated uncertainty to allow for real-time decisions.

During the last years, high drilling activity, use of permanent sensors for monitoring pressure and flow rates and developments in 4D seismic monitoring, have considerably increased the data output frequency of producing fields. Thus growing need for fast and continuous model updating calls for alternative solutions to traditional history matching methods, which are often unacceptably time-consuming. Sequential data assimilation appears ideally-suited for adressing the new challenges within reservoir management.

The Ensemble Kalman Filter (EnKF) was introduced by *Evensen* (1994) for updating non-linear ocean models. It is a Monte Carlo approach where errors are represented by an ensemble of realizations. The model parameters and state variables are updated sequentially in time, as new measurements become available. The result is an updated ensemble of realizations, conditioned to all production data, which provides an improved estimate of the model parameters, the state variables, and their uncertainty.

Since its first application within the pertroleum industry, several publications have discussed the use of the EnKF for parameter estimation in oil reservoirs, and have shown promising results. Nevertheless, most published papers present synthetic cases (e.g. *Nævdal et al.*, 2002, *Gu and Oliver*, 2005), while real field applications have only recently been considered. Previous works that demonstrate the capability to use the EnKF for history matching real reservoir models are *Skjervheim et al.* (2005), *Haugen et al.* (2006), *Bianco et al.* (2007), and *Evensen et al.* (2007). All these studies conclude that the EnKF is able to significantly improve the match of production data compared to manual history matching, and to provide improved estimate of model parameters. Previously, the focus has mainly been on the estimation of porosity and permeability fields in the simulation models. In *Evensen et al.* (2007), parameters such as initial fluid contacts, and fault and vertical transmissibility multipliers, are included as additional uncertain parameters to be estimated.

In this paper, the EnKF is presented as a method for history matching reservoir simulation models and discussed in relation to traditional methods where a cost function is minimized. The EnKF history matching workflow for applications in reservoir management projects is described in some detail. The properties of the EnKF are demonstrated in a real field application where it is illustrated how a large number of poorly known parameters can be updated and where the uncertainty is reduced and quantified through the assimilation procedure. It is shown that introduction of additional model parameters such as the relative permeability leads to a significant improvement of the results when compared with previous studies. Finally, the updated ensemble is used to predict the uncertainty in future production.

Assisted history matching

It is not intended to give a detailed discussion of the EnKF. There exists an extensive litterature and we refer to *Evensen* (2007) which gives a thorough presentation of the EnKF for solving the general state and parameter estimation problem. Instead, we present the EnKF as an alternative to traditional assisted history matching methods, and we present the practical implementation and EnKF general workflow for applications in oil reservoir projects.

Conditioning reservoir stochastic realizations to production data is generally described as finding the optimal set of model parameters that minimizes the misfit between a set of measurements and the corresponding responses calculated on the realization of the stochastic model. However, it can also be formulated in a Bayesian framework, as finding the posterior pdf of the parameters and the model state, given a set of measurements and a dynamical model with known uncertainties. From Bayes' theorem, the *posterior pdf* of a random variable ψ, conditional on some data d, is given by,

$$f(\psi|d) \propto \; p(\psi)p(d|\psi) \tag{1}$$

where $p(\psi)$ is the *prior pdf* for the random variable and $p(d|\psi)$ the *likelihood function* describing the uncertainty distribution in the data. This Bayesian formulation is the common starting point for traditional minimization methods and sequential data assimilation methods (Fig.1).

Traditional minimization methods

Starting from Bayes' theorem a general cost function can be defined by adopting Gaussian distributions for the prior random variables and the measurements. An additional assumption is often imposed where the dynamical model is treated as perfect and no model errors are accounted for. Furthermore the errors in the initial conditions are often neglected as well. These assumptions lead to a cost function which only measures the distance between the parameter estimate and its prior, plus the distance between the model solution and the measurements (Fig.1 A.2). Thus, only the parameters are solved for, and a given set of parameters defines a unique model solution. However, it is important to realize that we have now neglected other possible errors in the model and in the initial conditions.

The resulting quadratic cost-function is normally minimized using different kinds of descent methods (Fig.1 A.3.a). Typical methods involve the use of gradients where the gradient may be evaluated by solving the adjoint model (see e.g. *Evensen*, 2007). The solution obtained is a single realization which hopefully represents the global minimum of the cost function. With a single realization representing the solution there is no error estimate available.

A serious problem is that the cost function is highly nonlinear, and the parameter-estimation problem becomes

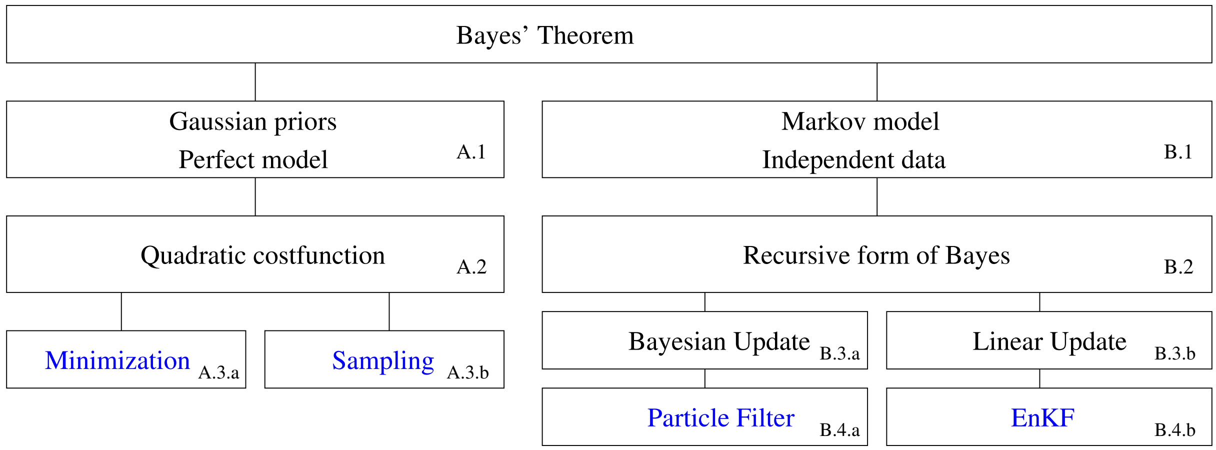

Figure 1: Bayes' theorem as a common starting point for assisted history matching methods. The left route illustrates how the assumptions of a Gaussian priors and a perfect model are needed to arrive at a minimization of a cost function for solving the inverse problem. The right route illustrates how the assumption of the model being a Markov process and that measurement errors are uncorrelated in time leads to a sequence of inverse problems that are well suited for ensemble methods. In a linear world the methods derived using the two routes will give identical results.

extremely challenging even with relatively few parameters to estimate. Using minimization methods the solution is searched for in a space with dimension equal to the number of poorly known parameters. The nonlinearities of the inverse problem lead to a cost function with multiple local minima. Thus, the probability of converging to a local minimum is high and in most realistic applications the global minimum is never found. It is also clear that the inverse problem becomes harder to solve for long time intervals since non-Gaussian contributions have more time to develop.

Thus, as an alternative to standard minimization, various sampling methods, have been proposed (Fig.1 A.3.b), which applies guided Monte Carlo sampling of the solution space. Sampling methods increase the likelihood for finding the global minimum but to an, often, unacceptable high numerical cost associated with the huge number of model simulations required when the dimension of the parameter space becomes large. If the global minimum can be found, the sampling methods, such as genetic algorithms (*Goldberg*, 1989) and Randomized Maximum Likelihood *Oliver et al.* (1996), also provide an estimate of the posterior pdf around the global minimum and an error estimate can be derived.

Sequential data assimilation

An alternative route is taken in *Evensen* (2007). Starting from Bayes' theorem two assumptions are made (Fig.1 B.1). First the simulator or dynamical model is assumed to be a Markov model, which means that the solution at one time-instant is only dependent on the solution at the previous time-instant. This property is normally satisfied for most time-dependent models. The second assumption is that the measurement errors are uncorrelated in time. This assumption is often implicitly used in methods that minimize a cost function, when a diagonal error covariance matrix is specified for the measurements.

As is discussed in *Evensen* (2007), the assumption of independent data in time allows for Bayes' theorem to be written as a recursion where data are processed sequentially in time and we end up with a sequence of inverse problems (Fig.1 B.2). Each of the inverse problems can be solved using any minimization method. However, to proceed in the recursion, access is needed to both the prior estimate and its uncertainty.

The particle filter by *Doucet et al.* (2001) is proposed as a general method for solving the sequence of inverse problems (Fig.1 B.4.a). The pdf for the solution is approximated by a large number of particles, or model states. Each of the model states are integrated forward in time according to the model equations, which include stochastic terms to represent model errors. At each time when data are available a Bayesian update is computed by re-sampling of the posterior distribution. The solution is a large ensemble of model realizations which represents the posterior pdf. The particle filter requires a large number of realizations to converge, and is so far only applicable to rather low dimensional problems.

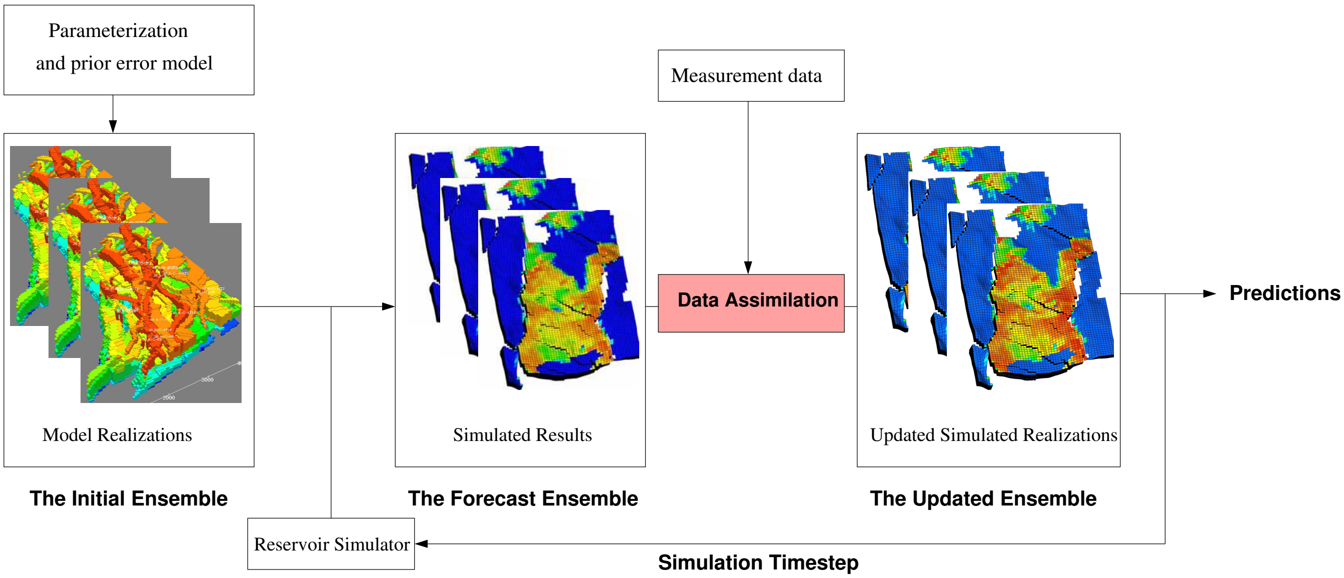

Figure 2: The general EnKF workflow for oil reservoir applications: The initial ensemble which expresses explicitly the model uncertainty is the starting point for the Ensemble Kalman filter. Forward integration of each ensemble member leads to the forecast ensemble. Updates are performed at each time when measurements of production data are available. These two processes, the forecast and the analysis, consist the main EnKF loop, leading to an updated ensemble.

The Ensemble Kalman Filter is to some extent similar to the particle filter, except that a simplification is imposed in the update step (Fig.1 B.4.b). It is assumed that the predicted prior pdf is well approximated using only the first and second order moments of the pdf. It is then possible to efficiently compute a linear update using the procedure outlined by *Evensen* (1994, 2007), where each realization is updated according to the standard Kalman filter update equation, but using measurements contaminated with simulated noise representing the measurement errors.

In the EnKF the sequential updating has the nice property of introducing Gaussianity into the pdf at each update step (see *Evensen*, 2007). The model solution is kept on track and is consistent with the data and true solution, and non-Gaussian contributions are not allowed to develop in the pdf. The implication is that the linear update step used in the EnKF in many cases is a reasonable and valid approximation. This fact does to a large extent explain the success of the EnKF in many nonlinear inverse problems.

EnKF history matching workflow

The history matching workflow, independent of the method used, involves three major steps; first a *parameterization* where the parameters that are uncertain and at the same time characterize the major uncertainty of the model solution are identified, thereafter a *prior error model* is specified for the selected parameters based on an initial uncertainty analysis, and finally a *solution method* needs to be selected. All three steps may be equally important and the selections and choices made will depend on the problem at hand.

Parameterization

Traditional methods for assisted history matching are constrained to include a low number of model parameters in the optimization process. The history matching process is then performed using only the most influential parameters, typically identified from a sensitivity study. Often aggregated parameters are used to reduce the number of parameters in the estimation, and an example can be a region pore volume multiplier.

The EnKF is, on the other hand, not limited by the number of model parameters. The reason is that the dimension of the inverse problem is reduced to the number of realizations included in the ensemble. Thus, the solution is searched for in the space spanned by the ensemble members rather than the high dimensional parameter space. It is however important that the major variability of the parameters can be represented by a number of modes that are of the same order as the number of realizations.

The typical uncertain elements to consider in a reservoir characterization study are: the structural model which is based on seismic time interpretation and time-to-depth conversion; petrophysical evaluation of wells and property mapping; depth of fluid contacts; horizontal and vertical barriers to fluid flow including vertical and horizontal permeability, and fault transmissibility. Currently, the structural framework is assumed deterministic in all our field cases. However, the geophysical and thus structural uncertainties are known to be significant in many reservoir models, but estimating structural parameters with the EnKF is still an unsolved problem, the major issue being that structural updates may change the model grid.

Prior error model

An initial uncertainty analysis leads to a quantification of the prior uncertainties of the parameters, which is then represented using pdfs. The specified pdfs then represent our prior belief concerning the uncertainty of each particular parameter. The priors must be defined to obtain a realistic relative weighting on the first guesses of parameters, the model dynamics, and the measured data.

A reservoir is normally characterized by a so called geological model that is built using a reservoir modelling software. The geological model should integrate all available prior information from 3D seismic surveys, core and log data, outcrop studies, and conceptual model. Stochastic simulations are used to produce multiple realizations of the porosity and permeability fields in the reservoir model. The multiple stochastic realizations then represent the uncertainty in the property model. The realizations are conditioned to the well observations and honour the statistical properties such as trends and spatial correlation of the well-log data. It is also possible to condition the properties on seismic data. The petrophysical realizations are then up-scaled to the simulation grid.

There is a large number of additional parameters that need to be specified in the simulation model, and most of these also have a non-negligible uncertainty associated with them. Some simulation model parameters previously estimated using the EnKF include fault transmissibility, horizontal and vertical barriers to fluid flow, and the initial vertical distribution of fluids in the model through the specification of the initial fluid contacts.

The uncertain parameters are normally characterized by a Gaussian distribution with mean equal to the best estimate and a standard deviation reflecting the uncertainty. Parameter values for the different realizations are then generated by random sampling from the prescribed distributions. The dynamic variables, pressure and saturation grid-cell values, are included in the initial ensemble through an initialization using the flow simulator.

Thus, when using the EnKF one first creates an ensemble of reservoir models expressing explicitly the model uncertainty (Fig.2 The Initial Ensemble). The ensemble mean is considered as the best estimate and the spreading of the ensemble realizations around the mean reflects the uncertainty in the estimate.

State vector

The state vector $\mathbf{\Psi}$ is a high-dimensional vector consisting of static parameters, dynamic variables, simulated production data and/or seismic data, and it is written as,

$$\mathbf{\Psi} = \begin{pmatrix} \boldsymbol{\psi} & \text{dynamic state variables} \\ \boldsymbol{\alpha} & \text{static parameters} \\ \boldsymbol{d} & \text{predicted data} \end{pmatrix}. \tag{2}$$

The 3D dynamic state variables include the fundamental variables in the flow simulation, such as the reservoir pressure P, the water saturation S_{w}, the gas saturation S_{g} as well as the solution gas-oil ratio R_{s} and the vapor oil-gas ratio R_{v}.

The static parameters consist of, for example, the 3D fields of porosity and horizontal and vertical permeability, fault transmissibility multipliers for each fault in the model, vertical transmissibility multipliers that regulate flow between various zones in the reservoir, the relative permeability parameterization as presented in this paper, and the depth of initial water-oil contacts and gas-oil contacts.

The predicted measurements are included in the state vector, since they are nonlinearly related to the model state and their inclusion in the state vector simplifies the comparison with the measured data in the EnKF update scheme. The predicted measurements are typically the oil, gas and water rates for each well, as well as the gas-oil ratio and the water cut. When 4D seismic data is used to condition the model dynamics, the predicted seismic response is also included in the state vector in some form (*Skjervheim et al.*, 2005).

Data assimilation and EnKF updating

Once an initial ensemble of reservoir models is generated, the EnKF is used to update the ensemble sequentially in time to honour the new observations at the time they arrive. The EnKF consists of a forward integration to generate *the forecast* followed by the updating of state variables to generate *the analysis* (Fig.2).

In the forecast step, the ensemble of reservoir models is integrated forward in time using the dynamical model. Each ensemble member is integrated until the next time when production measurements are available, leading to the forecast ensemble.

The assimilated observations $\boldsymbol{d}$ are considered as random variables having a distribution with the mean equal to the observed value and an error covariance $\boldsymbol{C}_{\epsilon\epsilon}$ reflecting the accuracy of the measurement. Thus, following *Burgers et al.* (1998) we generate an ensemble of observations $\boldsymbol{d}_j = \boldsymbol{d} + \boldsymbol{\epsilon}_j$ where $\boldsymbol{\epsilon}_j$ represents the measurement error and $\boldsymbol{C}_{\epsilon\epsilon} = \overline{\boldsymbol{\epsilon}\boldsymbol{\epsilon}^T}$ where the overline denotes the average over the ensemble.

In the analysis, the following updates are computed for each of the ensemble members,

$$\boldsymbol{\Psi}_j^{\mathrm{a}} = \boldsymbol{\Psi}_j^{\mathrm{f}} + \boldsymbol{C}_{\psi\psi}\boldsymbol{M}^{\mathrm{T}}(\boldsymbol{M}\boldsymbol{C}_{\psi\psi}\boldsymbol{M}^{\mathrm{T}} + \boldsymbol{C}_{\epsilon\epsilon})^{-1}\,(\boldsymbol{d}_j - \boldsymbol{M}\boldsymbol{\Psi}_j^{\mathrm{f}}), \tag{3}$$

where $\boldsymbol{\Psi}_j^{\mathrm{f}}$ represents the state vector for realization j after the forward integration to the time when the data assimilation is performed, while $\boldsymbol{\Psi}_j^{\mathrm{a}}$ is the corresponding state vector after assimilation. The ensemble covariance matrix is defined as $\boldsymbol{C}_{\psi\psi} = \overline{(\boldsymbol{\psi} - \overline{\boldsymbol{\psi}})(\boldsymbol{\psi} - \overline{\boldsymbol{\psi}})^{\mathrm{T}}}$, where $\overline{\boldsymbol{\psi}}$ denotes the average over the ensemble. The matrix $\boldsymbol{M}$ is an operator that relates the state vector to the production data and $\boldsymbol{M}\boldsymbol{\Psi}_j^{\mathrm{f}}$ extracts the predicted or simulated measurement value from the state vector $\boldsymbol{\Psi}_j^{\mathrm{f}}$.

The updated ensemble is then integrated until the next update-time. The result is an updated ensemble of realizations, conditioned to all previous production data, and thus the optimal starting point for predictions of future production.

Estimation of relative permeability

Relative permeability is defined as the ratio of effective permeability of a particular fluid at a particular saturation (i.e. in presence of another fluid) to the absolute permeability of the porous medium at single phase saturation. In a heterogeneous medium, where relative permeability properties are derived from core-samples and may not be representative at the reservoir scale, history matching of up-scaled relative permeability curves may lead to improved results. The relative permeability curves obtained from the core laboratory experiments should not be directly used in the reservoir simulation model, but need to be up-scaled to compensate for fluid forces, numerical dispersion, and geological heterogeneity effects. Unfortunately, the up-scaling techniques require large computational time and may not be robust. Therefore, our approach is to obtain relative permeability properties directly at the coarse scale by data assimilation. Hence, estimating the shape of relative permeability curves at the coarse scale are closely related to the up-scaling issues and the lack of information of the fine scale permeability heterogeneity.

Several recent publications show the potential of estimating relative permeability properties on a coarse scale reservoir simulation model. In *Okano et al.* (2005) the authors adjust the relative permeability curves during history matching using the neighbourhood approximation algorithm, where they use different parameterization schemes. The method is applied on synthetic cases, and the results show that they are able to match the production data by adjusting the relative permeability curves. *Eydinov et al.* (2007) use an adjoint method to perform a simultaneous estimation of absolute and relative permeability by automatic history matching of three-phase flow production data.

In this paper, we include the relative permeability as an uncertain parameter to be estimated in the EnKF. We employ Corey functions (*Brooks and Corey*, 1964) to parameterize coarse scale relative permeability curves. The Corey parameterization is flexible and is often used in the petroleum industry. According to this model the relative permeability in an oil-water system is given by

$$k_{\mathrm{rw}} = k_{\mathrm{rw}}^{\star}\left(\frac{S_{\mathrm{w}} - S_{\mathrm{wc}}}{1 - S_{\mathrm{wc}} - S_{\mathrm{orw}}}\right)^{e_{\mathrm{w}}}, \tag{4}$$

$$k_{\mathrm{row}} = k_{\mathrm{row}}^{\star}\left(\frac{1 - S_{\mathrm{w}} - S_{\mathrm{orw}}}{1 - S_{\mathrm{wc}} - S_{\mathrm{orw}}}\right)^{e_{\mathrm{ow}}}, \tag{5}$$

where $k_{\rm rw}$ is the water relative permeability and $k_{\rm row}$ is the oil relative permeability. The relative permeabilities in an oil-gas system are given as

$$k_{\rm rg} = k^{\star}_{\rm rg}\left(\frac{S_{\rm g} - S_{\rm gc}}{1 - S_{\rm wc} - S_{\rm gc} - S_{\rm org}}\right)^{e_{\rm g}}, \tag{6}$$

$$k_{\rm rog} = k^{\star}_{\rm rog}\left(\frac{1 - S_{\rm g} - S_{\rm org}}{1 - S_{\rm wc} - S_{\rm gc} - S_{\rm org}}\right)^{e_{\rm og}}. \tag{7}$$

where $k_{\rm rg}$ is the gas relative permeability and $k_{\rm rog}$ is the oil relative permeability.

In a three phase system, the three phase oil relative permeability at a particular water and gas saturations is extrapolated from the input two phase relative permeability model.

Large flexibility in the relative permeability parameterizations is important, and the following parameters in the Corey function can be updated in the data assimilation; the relative permeability end points $k^{\star}_{\rm rg}$, $k^{\star}_{\rm rog}$, $k^{\star}_{\rm row}$, $k^{\star}_{\rm rw}$, the Corey exponents $e_{\rm w}$, $e_{\rm ow}$, $e_{\rm g}$, $e_{\rm og}$, the connate water and gas saturation $S_{\rm wc}$, $S_{\rm gc}$, and the residual oil and gas saturation $S_{\rm orw}$, $S_{\rm org}$. In the current implementation the connate gas saturation is equal to the critical gas saturation, and the connate water saturation is equal to the critical water saturation.

Transformed fault transmissibility multipliers

Faults can act as both barriers and conduits to fluid flow, and are normally included in reservoir-simulation models as grid offset and using 2D transmissibility multipliers. The fault transmissibility multipliers should be limited to the interval $[0, 1]$, where a numerical value of 0 reflects a complete flow barrier and a value of 1 characterizes an open fault. The upper bound can be relaxed in many simulators without much influence on the flow properties. Anything in between 0 and 1 corresponds to a partial barrier to fluid flow. Experience shows that a large change in the fault transmissibility is needed to obtain significant changes in the flow behaviour. Note also that the transmissibility needs to be almost identically zero to maintain a difference in the pressure across the fault.

There are generally large uncertainties associated with the fault fluid-flow properties and faults transmissibility multipliers have already been included as parameters to be estimated using the EnKF in *Evensen et al.* (2007). In their field application, the prior guess for the uncertain multipliers is set to 1.0, with a standard deviation of 0.2. Results from the EnKF assimilation show that the uncertainty of the multipliers is not significantly reduced and it is concluded that the production is not very sensitive to this parameter. Similarly, we estimated the fault multipliers using a Gaussian distribution to reflect the uncertainty. However, only small updates of the order 0.20 to 0.35 were obtained and it is impossible to determine whether a fault is closed or open, which is often the level of uncertainty. The use of appropriate transformations to some extent enables us to overcome the bottleneck linked to updating non-Gaussian variables in the EnKF. With this concept, the EnKF updates a Gaussian variable, which is transformed before it is used in the reservoir simulator. The following transformation gives satisfactory results and is used in our field studies for updating faults as well as vertical transmissibility multipliers,

$$y = \frac{1}{\sqrt{2\pi}\sigma}\int_{-\infty}^{x} dt\, \mathrm{e}^{-\frac{(t-\mu)^2}{2\sigma^2}}, \text{ with } x \sim N(0, 1). \tag{8}$$

The transformation (8) ensures that the output variable y is in the range $(0, 1)$ and, depending on the values of the variables σ and μ, it is possible to get either a reasonably uniform distribution, a bimodal distribution with peaks close to 0 and 1, or a uni-modal distribution peaked around a value in $(0, 1)$.

Field Case

The proposed workflow based on the EnKF has been applied to history match several North Sea simulation models. The results from a complex real field case is presented and discussed below.

Reservoir presentation

The Omega field is part of a larger North-South elongated fault block, and has a length of approximately 8 km and a width between 2.5 and 3.5 km. The structure represents an open synform and is bounded by faults, which are assumed to be sealing. The main reservoir consists of shallow-marine deposits and associated near-shore, deltaic

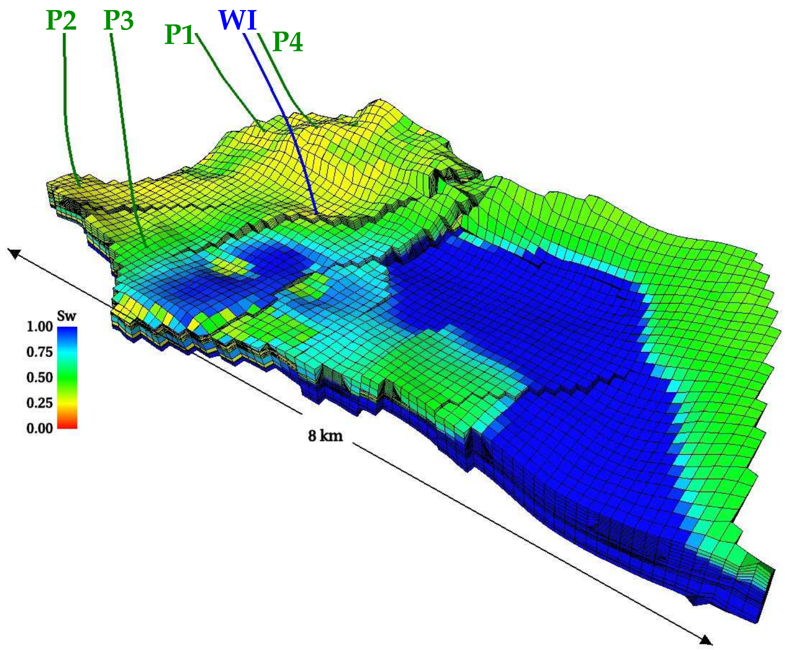

Figure 3: The Omega field initial water saturation. Four horizontal producers (P1 to P4) drain the northern part of the field, while a vertical water injector (WI) ensures pressure support.

sediments. High spatial and temporal variations are the consequences of a succession of transgressive-regressive events combined with syn-sedimentary fault activity. The architectural style is complex, flow properties are heterogeneous and vertical communication is relatively poor.

Numerous faults lead to considerable structural complexity. The understanding of the fault network is to some extent guided by interpretations of water-oil contacts (WOC), although original observations of WOC's are rare, thus primarily based on pressure gradient analysis. Fluid contacts controlling mechanisms are poorly understood and fault properties are highly uncertain.

The reservoir was initially at saturated conditions. The presence of a small gas cap in the north of the structure is interpreted as resulting from gas migration from the west. The field was set in production in 2000 and is drained by four horizontal producers and one water injector ensuring pressure support. Water injection started in 2004.

The simulation grid consits of 37×80 cells, with a lateral spacing of 100×100 m, and 40 layers with varying thickness. A total of 60 000 cells were active in the simulation.

The initial ensemble

The method described in the section "EnKF history matching workflow" was used to build the initial ensemble. The focus was set on the target reservoir, located between layers 17 and 40. The main uncertain parameters identified in the Omega model are porosity and permeability fields, depths of initial fluid contacts, relative permeability and fault multipliers.

The porosity and permeability distributions are derived from analysis of well-log data. Due to spurious permeability measurements in the horizontal producing wells, it is decided not to constrain the Omega model to the well-log data from any of the four producing wells. Only the well-log data from the appraisal wells and the water injector are used. The geo-statistics from the initial ensemble are summarized in Table 1. Note that the upper part of the model (layers 1 to 16) is not assigned any uncertainty. A deterministic correlation coefficient of 0.7 between porosity and permeability and a vertical to horizontal permeability ratio of 0.1 are assumed. The fields resulting from the geostatistical simulation are then up-scaled to the simulation grid.

The Omega structure is divided into five different equilibrium regions each having individual water-oil and gas-oil contacts. The prior means of the contacts are derived from well-log interpretations and by pressure analysis, and the standard deviation of the contacts is set to 5 m.

The initial coarse-scale relative permeability curves, generated from special core analysis measurements and

Layers	Porosity mean (std)	Permeability mean (std)	Azimut	Correlation X(Azimut),Y	Vert. corr.
17-26	0.16 (0.03)	65 (86)	0	3000,3000	5
27-28	0.20 (0.03)	910 (1085)	60	2000,600	5
29-30	0.23 (0.03)	292 (397)	160	1500,1000	25
31	0.14 (0.04)	4.6 (4)	340	1000,500	5
32-33	0.16 (0.05)	10 (40)	340	1000,500	25
34-35	0.23 (0.03)	300 (350)	340	1500,1000	5
36	0.06 (0.03)	6 (30)	0	1000,1000	5
37	0.05 (0.03)	39 (20)	0	1000,1000	5
38-39	0.19 (0.04)	47 (190)	60	2000,600	25
40	0.10 (0.01)	8 (22)	60	2000,1000	5

Table 1: Geomodel statistics properties.

Parameter	Mean	Std.dev
$k_{rw}^{\star}$	0.6	0.05
e_w	3	0.5
e_{ow}	4	0.5
e_g	1.8	0.5
e_{og}	5.4	0.5
S_{wc}	0.25	0.05
S_{gc}	0	0.02
S_{orw}	0.18	0.05
S_{org}	0.05	0.03

Table 2: Relative permeability prior statistics.

adapted to Corey curves, have been used as the initial prior in the EnKF. For simplification, only one set of relative permeability properties is defined for the whole field in the current experiment. The initial values for the critical saturations are then defined as the best guess averaged field values. Table 2 presents the parameters in the Corey function that were updated in the data assimilation and associated statistics. It should be mentioned that the relative permeability in the Omega model has previously not been considered as a history matching parameter.

Interpretation of the fault transmissibility properties has to some extent been guided by pressure measurements and inferred from sensitivity studies. A large uncertainty nevertheless remains. For faults without any prior knowledge about the behavior with respect to flow, we have used values $\sigma = 1$ and $\mu = 0$ leading to a prior fault transmissibility multiplier that is uniformly distributed between 0 and 1. A few faults are known to be pressure barriers, thus, the value of μ is increased to lead to a distribution of fault multipliers skewed towards zero. A total of 7 fault multipliers is estimated and the total number of variables to update is over 200 000.

The production data considered in the history matching are monthly averaged oil-production rates, water rates and gas rates from each well. The history-matching period covers 6 years. The measurement uncertainty is specified as a percentage of the measured rate. We have used 10 % of the measured value for the oil rate, 15 % for the gas rate and 20 % for the water rate. In the simulation, all wells are controlled by specifying a target for the reservoir-fluid volume-rate.

Results

Validation of updated models The results from the EnKF history match are shown in Figures 4 to 5, where we have plotted the oil production total (OPT), the oil production rate (OPR), the gas-oil ratio (GOR) and the water cut (WCT) for well P2 and P3. The blue curves represent 20 realizations of the prior ensemble, unconditioned to production data. The red curves are from a rerun of the 20 ensemble members when initialized with the EnKF updated parameters. The black dots represent the observations.

The initial uncertainty on the model parameters leads to a significant uncertainty in the simulated productions, which is illustrated by the prior spread in cumulative oil production for each well. For all the producers the EnKF

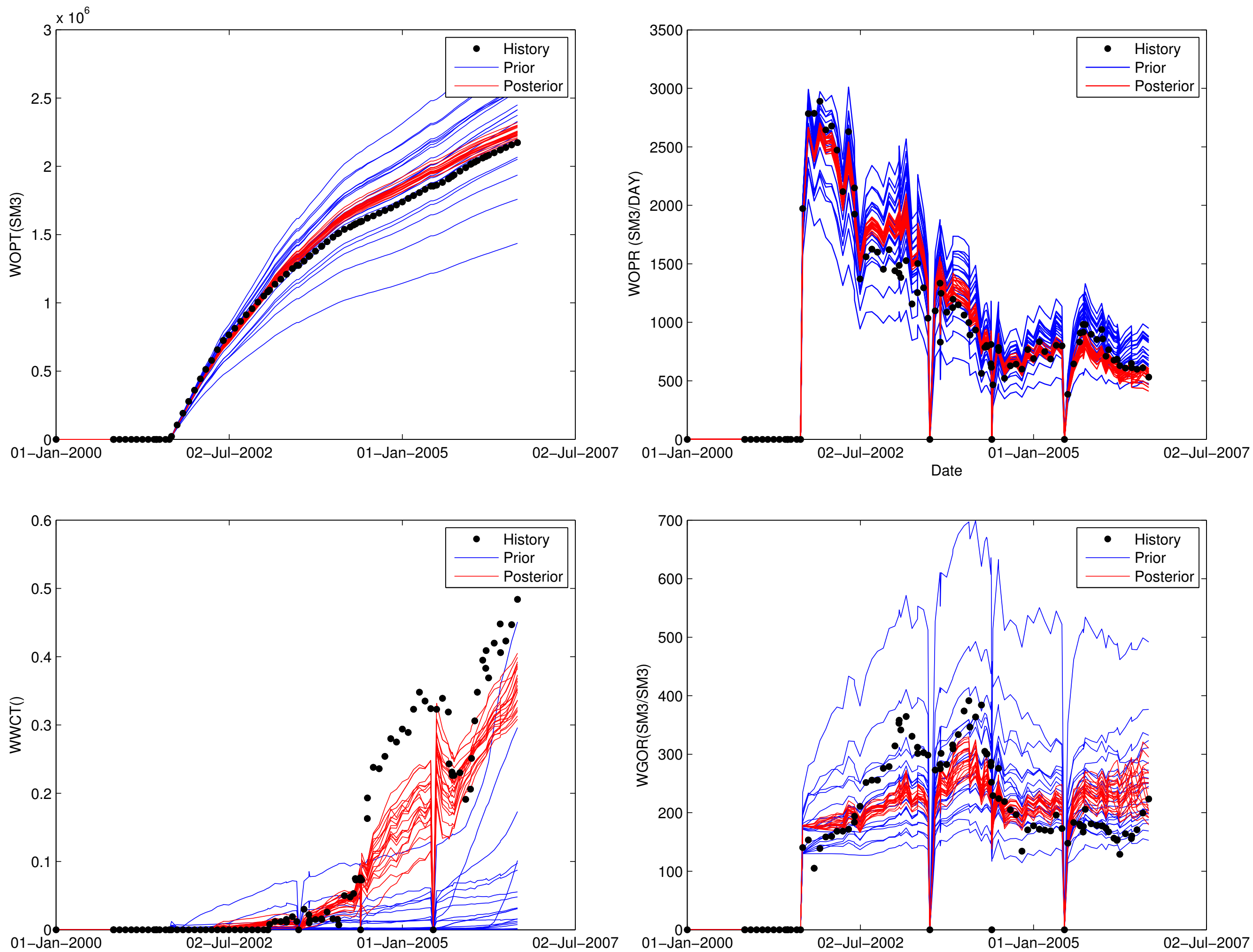

Figure 4: Well P2: Ensemble prediction based on prior ensemble of parameters (blue lines) and EnKF estimated parameters (red lines). Black dots are measurements.

updated ensemble manages to reproduce the observed data much better than the prior ensemble and the uncertainty is significantly reduced. It has previously been a challenge to obtain a satisfactory match of the water production in the Omega structure, and the reservoir models have had a poor prediction of the water breakthrough. The results from the EnKF illustrate that constraining the prior model on production data enables to capture the water production more accurately in all the wells. The improvements in wells P2 and P3 are satisfactory, as these have been very difficult to match manually. GOR observations are also reasonably reproduced.

Porosity and permeability updates It can be challenging to get an overall picture of the updates of the porosity and permeability fields by scrolling through the 100 different realizations, layer by layer. The applied modifications are maybe best analysed by comparing the initial and updated average fields, as well as the standard-deviation fields.

In Figure 6 we have plotted the initial and updated average porosity field for one layer, and in the lower part the corresponding standard deviation. The initial standard-deviation field shows that the northern part of the model domain, with low standard deviation (0.015), has been constrained to well-log data, whereas the southern part of the reservoir, with higher standard deviation (around 0.03), has not been constrained by well-log data. The updated porosity field shows only a small modification in the northern part, but we notice an important decrease in the average porosity at the toe of well P3. Furthermore, the final standard deviation is greatly reduced in this region, indicating that the updates can be interpreted with confidence.

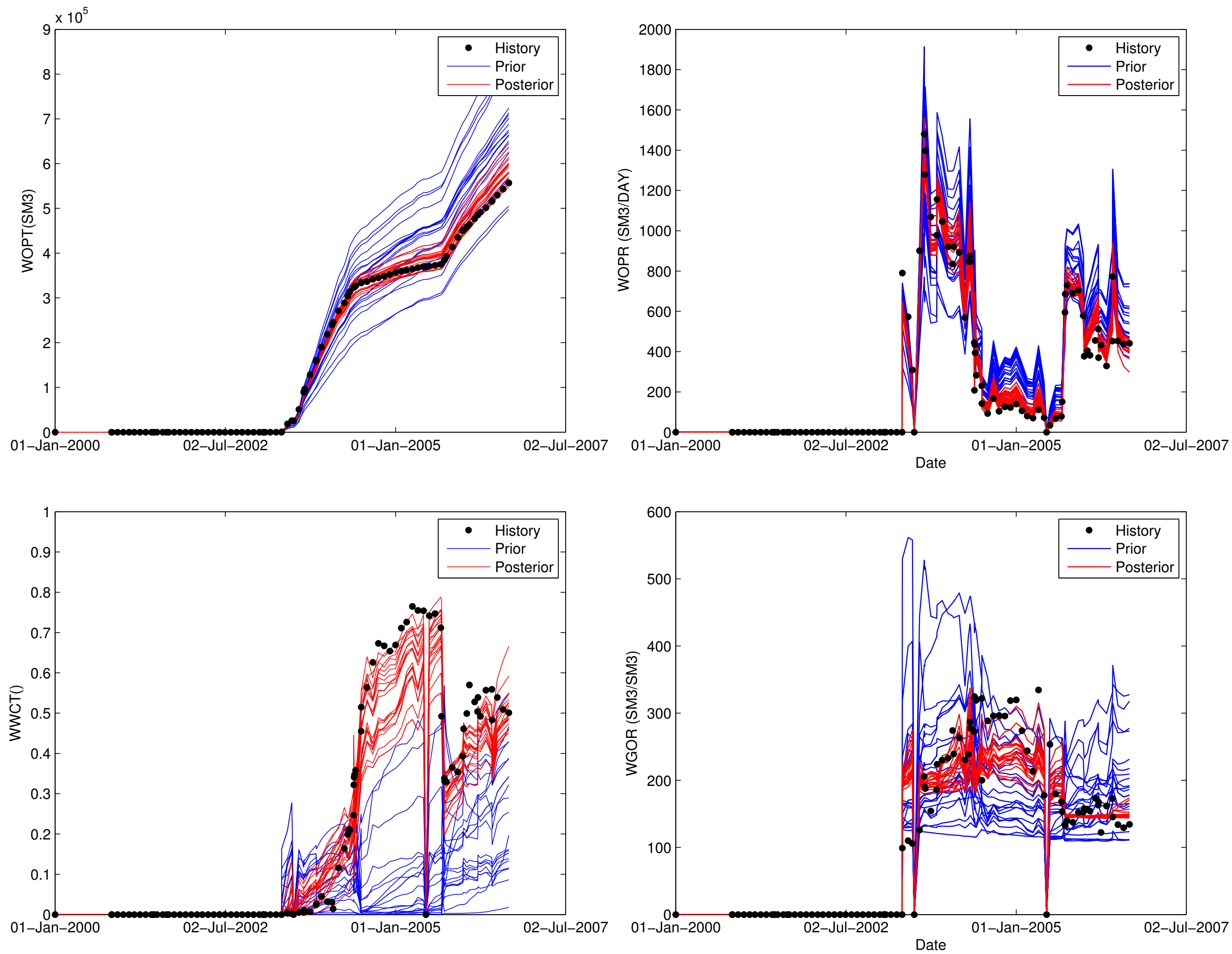

Figure 5: Well P3: Ensemble prediction based on prior ensemble of parameters (blue lines) and EnKF estimated parameters (red lines). Black dots are measurements.

The average field updates clearly show that an increase in porosity corresponds to an increase in permeability. This is reflecting the correlation coefficient (0.77) used when generating the prior realizations. Thus, updates in the petrophysical parameters will mainly impact the reservoir volumes and only to a minor extent the water or gas breakthrough time at the wells. The relative-permeability updates have the major impact on controlling the breakthroughs.

Relative permeability updates The strong updates in the parameters demonstrate that the relative permeability properties are important parameters to consider in the Omega model. The left plot in Figure 7 shows the initial (blue) and updated (red) water/oil relative permeability curves. The results indicate clearly that for high water saturation ($S_{\rm w} > 0.5$) the water mobility is increased. As a result, water breakthrough will occur faster. On the contrary the mobility at lower saturation is reduced, due to an increase in the critical water saturation. Thus, the initial water in the oil zone will be less mobile. The oil curve shows similar behaviour. The mobility at high oil saturation is increased, but more oil is left behind as a result of a higher residual oil saturation. The updated estimate of the residual oil saturation (0.36) is in accordance with the fractional flow curve obtained from core flooding experiments, which indicates that the residual oil after water flood is minimum 35%.

The right plot in Figure 7 shows the initial (blue) and updated (red) oil/gas relative permeability curves. The gas exponent is very sensitive to the well observations and the uncertainty is reduced. The gas mobility is increased.

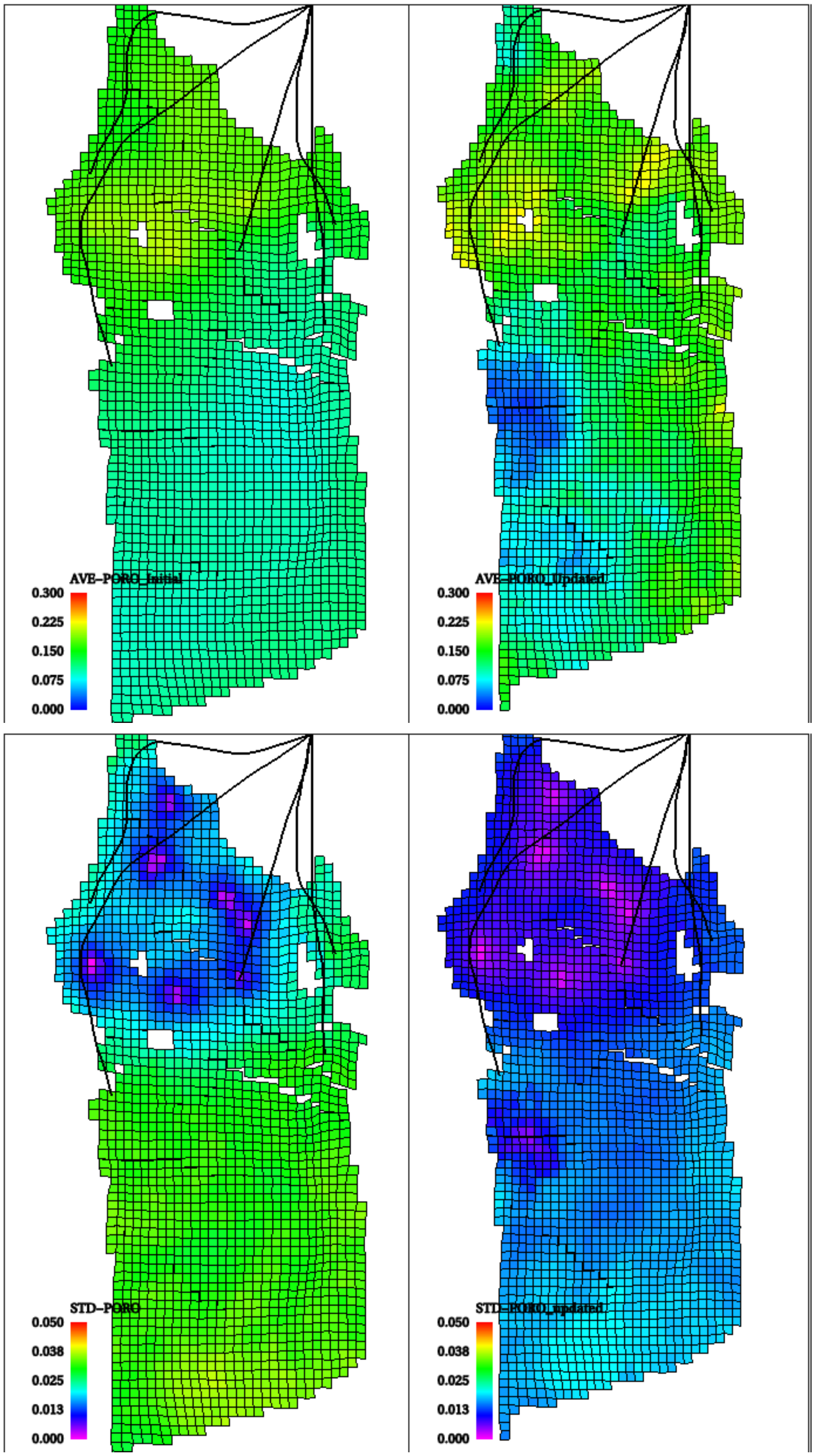

Figure 6: EnKF updates of porosity in a representative layer. Upper row; initial (left) and updated (right) average porosity in layer 19. Lower row; corresponding standard deviation, initial (left) and updated (right). Black lines show well paths of producers and injector.

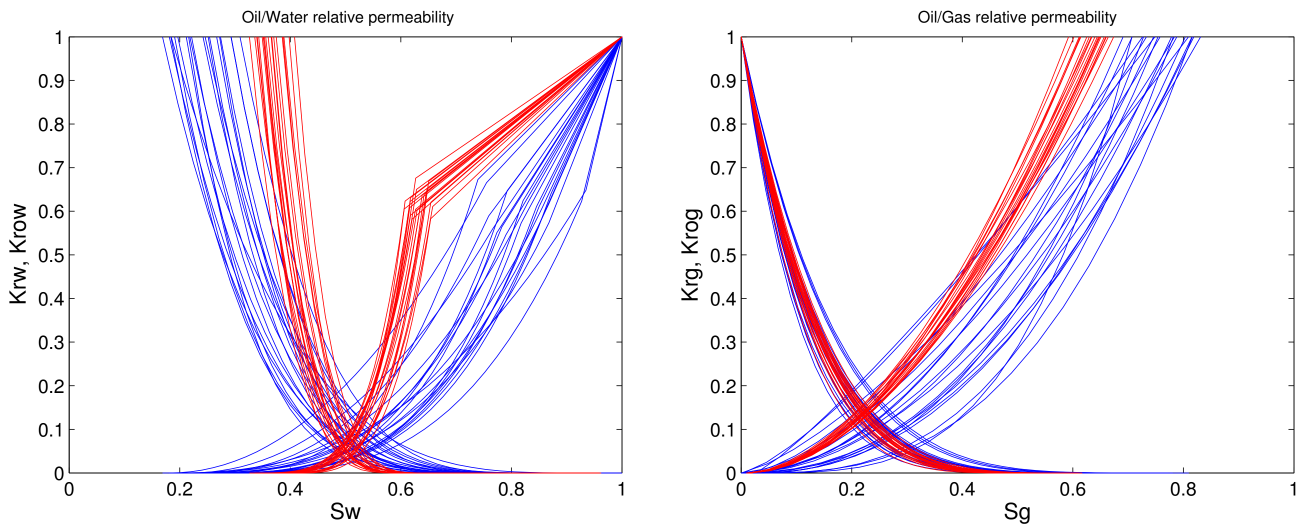

Figure 7: EnKF updates of relative permeability curves. Left; water/oil relative permeability. Right; gas/oil relative permeability. The blue lines show the initial uncertainty and the red lines the updated uncertainty.

The residual oil in presence of gas (S_{org}) is updated from 0 to 0.05 and the oil to gas exponent is decreased from 5.4 to 4.25. The EnKF updates are in line with conclusions drawn by the asset team where it is reported that this exponent is probably too high.

It is stressed that the updated curves should be considered as up-scaled curves, accounting for numerical dispersion and geological heterogeneity effects and thus, they will naturally differ from the measured properties on core samples, particularly in a heterogeneous medium. Furthermore, as mentioned earlier, a simplification was introduced by defining only one set of relative permeability curves for the whole field. In the reference case, one set of curves is defined per cell, the end-points being a function of the cell porosity, permeability and height above the fluid contact.

The permeability and relative permeability are indirectly linked, both controlling in some way the mobility of the fluids. In the current experiment we obtained an increase in both the relative permeability curves and the permeability field in the model. We also have some indications that the prior values of the permeability field may be too low (some well-log data have been excluded when building the initial ensemble) and this may then be compensated by too high values of the relative permeability curves. Thus, the prior permeability field should be revised.

Fault transmissibility multiplier updates The locations of the history-matched faults are illustrated in Figure 8. The sequential updating of the fault transmissibility multiplier is plotted in Figure 9 for the faults D, E and F.

For fault D, the initial distribution the fault transmissibility multiplier is skewed towards zero. During the assimilation the spread of the prior ensemble is significantly reduced, indicating that the assimilated data are strongly correlated with the transmissibility multiplier, and furthermore, that the updates can be interpreted with confidence. The updated ensemble clearly indicates a closed fault, which is in line with an observed pressure difference that is maintained across the fault.

The simulated production data are not significantly sensitive to the fault multipliers for faults C, B, and E, and for these faults the ensemble spread remains throughout the data assimilation, possibly due to the larger distance to the production wells. Thus, one should be careful in interpreting the results from these faults.

The variance is reduced for the fault F, which is located in the toe region of P3, and fault A, crossing well P2, and the updated ensemble suggests that these faults are not completely sealing but nevertheless act as a barrier to flow.

Sensitivity

In an earlier experiment where the relative permeability was not updated, the initial ensemble could not capture the water breakthrough and the updated ensemble was not able to correct for this initial bias. The updated water cut profile indicated that the injection water did not reach the well and in order to match the high WCT values observed near the end of the simulation, more formation water was mobilized by reducing the depth of the WOC. Subsenquently, when rerunning the reservoir simulator from time zero using the final updated parameters, the EnKF

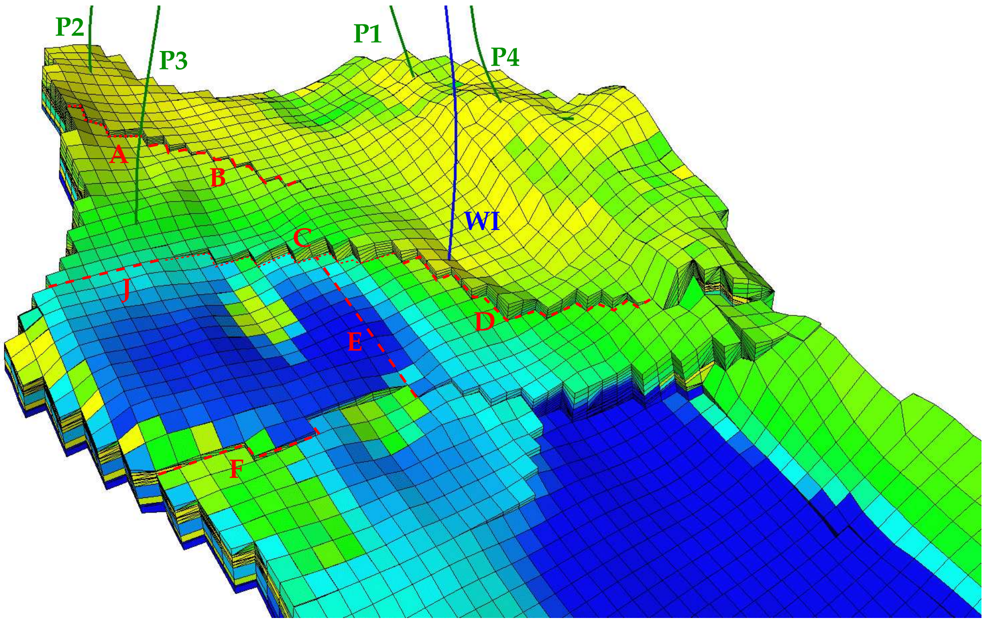

Figure 8: The location of the history-matched faults (red-dashed lines).

ensemble gives too early breakthrough times. This highlights the importance of the parameterization to obtain a good history match.

It is also worth mentioning that similar bias in the simulation performances were obtained by the asset team, working with a new model, based on an improved structural interpretation as well as a detailed facies model. Therefore, the additional updating of the relative permeability properties as well as the fault transmissibility multipliers appears to be a crucial element in order to capture the reservoir flow behaviour.

Predictions

Results presented so far demonstrate the potential and advantages of the EnKF as a history matching tool, its capability of handling large parameter spaces, and to provide an improved estimate of the model parameters the state variables and their uncertainty. But probably the most outstanding feature of the EnKF is the fact that it considers the combined parameter and state estimation problem. Thus the final updated ensemble can be used to perform predictions with uncertainty estimates, without the need to reintegrate the whole history.

In our field application, production data is assimilated until September 2006 and predictions are run into 2008. The prediction period was simulated by using a specified target liquid rate per well. The results for the oil production rate and water cut of well P2 are shown in Figure 10. The blue lines represent the Kalman filter update for the ensemble over the historical period and the green lines are the predictions starting from the final updated ensemble. Actual measurements are shown as black crosses. Predictions from the updated ensemble when assimilating only until January 2005 are also shown for comparison.

These predictions with uncertainty estimates provide the reservoir management teams with valuable information. Different production schemes and drainage strategies can be evaluated as well as the associated risk. Decisions are no longer based on a single basecase model.

Comparing the prediction profiles from January 2005 and September 2006 illustrates how the quality of the model continuously improves with time. The uncertainty in the prediction is reduced when more production data is assimilated. Comparison with the actual measurements (black crosses) allows some kind of validation of the predictions and the updated ensemble. Although these results are not direclty comparable since the actual observations also reflect the various workovers and choke manipulation at the plateform. The discontinuity between the EnKF update and the start of the prediction is interpreted as an expression of remaining bias in the model.

Figure 11 compares the predictions from the last data assimilation (green lines) with those obtained by reruning the simulator from time zero using the updated model parameters (red lines). Consistency has been established only

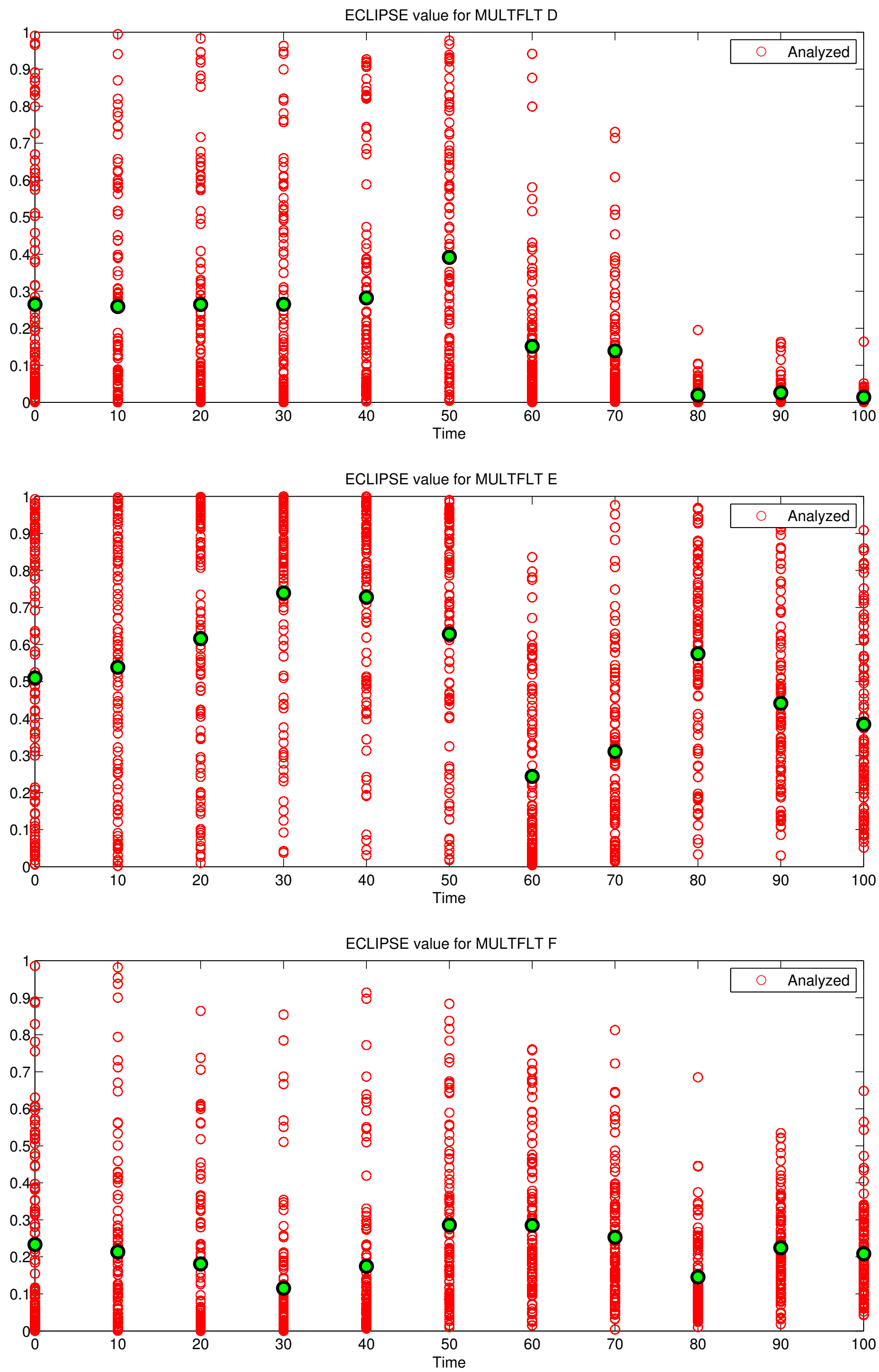

Figure 9: Sequential update of the fault transmissibility multiplier for faults D (upper plot), E (middle plot), and F (lower plot). The green circle indicates the ensemble mean.

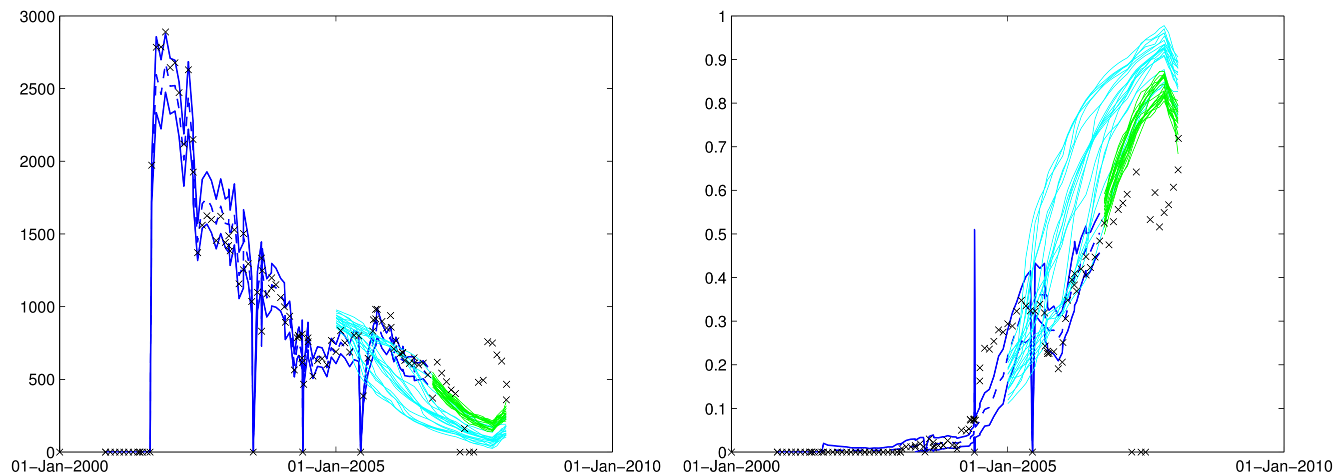

Figure 10: Well P2 predictions for oil rate (left) and water cut (right). Predictions from two different timesteps are compared: starting with the updated ensemble from January 2005 (cyan lines) and from September 2006 (green lines). Blue lines represent the Kalman filter update (mean ± 2 std) Black crosses are measurements.

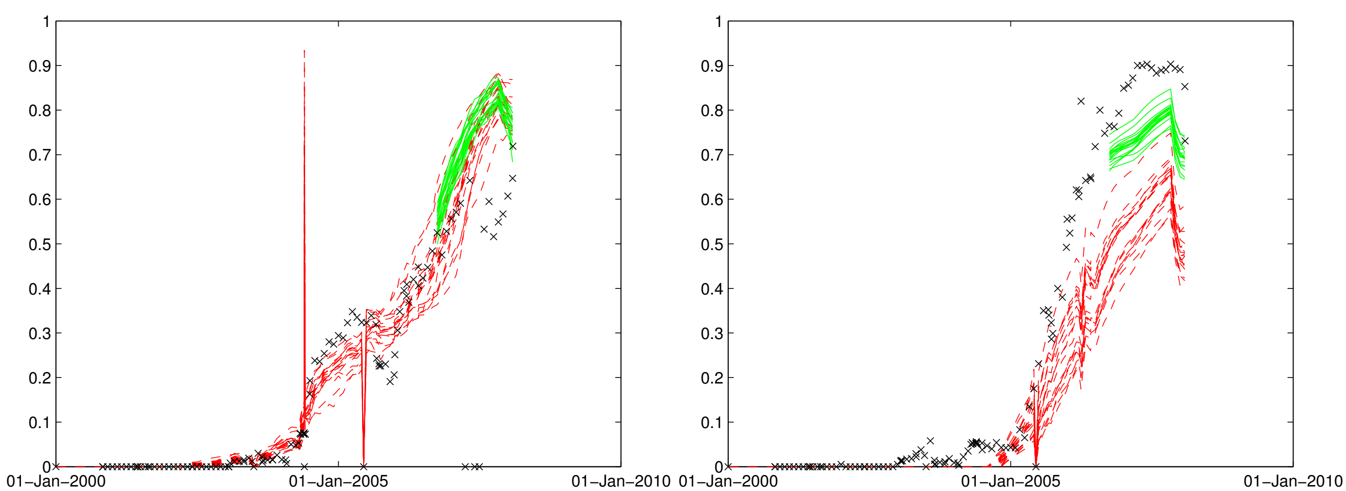

Figure 11: Comparing the predictions from the last data assimilation (green) with those obtained by rerunning the simulator from time zero with the updated parameters (red). Water cut profiles for well P2 (left) and P4 (right).

for linear dynamical systems where the predicted data is linearly related to the state vector. It provides in our case a validation of the updated parameters, particularly the depths of initial fluid contacts as these do not influence the predictions during the assimilation. Predictions from time zero using the updates values of the depths of initial fluids contacts versus predictions from the final updated state and parameters are consistent for the producer P2, located on the western flank of the structure. On the other hand, results for producer P4 on the eastern flank of the structure show inconsistencies and indicate that more accurate predictions will be obtained by simply making predictions from the last data assimilation time. These inconsistencies reveal that problems remain in the model, which could be linked to the omission of some important parameters, as for example the structural model.

Conclusions

A thorough workflow for updating reservoir simulation models using the EnKF is presented and demonstrated through a successful North Sea field case application.

The potential and advantages of the EnKF as an assisted history matching tool is demonstrated based on its capability of handling large parameter spaces, its sequential processing of measurements, and on the fact that it solves the combined state and parameter estimation problem as derived from a fundamental Bayesian formulation.

The EnKF provides an ensemble of updated reservoir realizations conditioned to production data, as well as improved estimates of the model parameters, the state variables, and their uncertainty. It forms an optimal starting point for computing predictions with uncertainty estimates.

It is demonstrated that estimating on relative permeability properties significantly improves the history match. It is concluded that the relative permeability is an important parameter to consider in the Omega model but also more generally. Updating relative permeability properties by production data assimilation allows to account for fluid forces, numerical dispersion and geological heterogeneity effects. In the presented field case, only one set of relative permeability curves was defined for the entire model. In the future, it might be valuable to differentiate between different regions, as well as horizontal versus vertical curves.

An improved parameterization for updating the fault transmissibility multipliers based on the use of transformations is presented. It is shown how the transformation enables us to successfully determine if a specific fault is open, closed or partially sealing with respect to flow.

References

Bianco, A., Cominelli, A., Dovera, L., Naevdal, G. and Valles, B. 2007. History Matching and Production Forecast Uncertainty by means of the Ensemble Kalman Filter: a Real Field Application. Paper SPE 107161 presented at the SPE Europec/EAGE Annual Conference and Exhibition, London, 11-14 June.

Brooks, R. H., and Corey, A. T. 1964. Hydraulic properties of porous media, *Hydrolo. Pap. 3*, civ. Eng. Dep., Colo. State Univ., Fort Collins.

Burgers, G., van Leeuwen, P. J., and Evensen, G. 1998. Analysis scheme in the ensemble Kalman filter, *Mon. Weather Rev.*, **126**: 1719–1724.

Doucet, A., de Freitas, N., and Gordon, N. (Eds.) 2001. *Sequential Monte Carlo Methods in Practice*, Statistics for Engineering and Information Science, Springer-Verlag New York.

Evensen, G., 1994. Sequential data assimilation with a nonlinear quasi-geostrophic model using Monte Carlo methods to forecast error statistics, *J. Geophys. Res.*, **99**:10,143–10,162.

Evensen, G., 2007. *Data Assimilation: The Ensemble Kalman Filter*, Springer-Verlag Berlin Heidelberg.

Evensen, G., Hove, J., Meisingset, H., Reiso, E., Seim, K., and Espelid, Ø. 2007. Using the EnKF for Assisted History Matching of a North Sea Reservoir Model. Paper SPE 106184 presented at the SPE Reservoir Simulation Symposium, Woodlands, 26-28 February.

Eydinov, D., Gao, G., Li, G., and Reynolds, A. C. 2007. Simultaneous estimation of relative permeability and porosity/permeability fields by history matching prediction data. Canadian International Petroleum Conference, Calgary, 12-14 June.

Goldberg, D. E., 1989. *Genetic Algorithms in Search, Optimization and Machine Learning*, Addison-Wesley Longman Publishing Co., Inc., Boston, MA, USA.

Gu, Y., and Oliver, D. S. 2005. History Matching of the PUNQ-S3 reservoir model using the ensemble Kalman filter. *SPE journal*, **10**(2):217–224.

Haugen, V., Natvik, L.-J., Evensen, G., Berg, A., Flornes, K., and Nævdal, G., 2006. History Matching using the Ensemble Kalman Filter on a North Sea Field Case. Paper SPE 102430 presented at the SPE Annual Technical Conference and Exhibition, San Antonio, 24-27 September.

Nævdal, G., Mannseth,T., and Vefring, E. 2002. Near well reservoir monitoring through ensemble Kalman filter. Paper SPE 75235 presented at the SPE/DOE Improved Oil Recovery Symposium, Tulsa, 13-17 April.

Okano, H., Pickup, G. E., Christie, M. A, Subbey, S., and Monfared, H. 2005. Quantification of Uncertainty in Relative Permeability for Coarse-Scale Reservoir Simulation. Paper SPE 94140 presented at the SPE Europec/EAGE Annual Conference, Madrid, 13-16 June.

Oliver, D. S., He N., and Reynolds A. C. 1996. Conditioning permeability fields to pressure data, Paper presented at the 5th European Conference for the Mathematics of Oil Recovery, Leoben, 3-6 September.

Skjervheim, J.-A., Evensen, G., Aanonsen, S. I., Ruud, B. O., and Johansen,T. A. 2005. Incorporating 4D Seismic Data in Reservoir Simulation Models Using Ensemble Kalman Filter. *SPE journal*, **12**(3):282–292.